

A COMPARATIVE STUDY OF METALLIC ADDITIVE MANUFACTURING POWER CONSUMPTION

M. Baumers*, C. Tuck*, R. Hague*, I. Ashcroft* and R. Wildman*

*Additive Manufacturing Research Group, Wolfson School of Mechanical and
Manufacturing Engineering, Loughborough University, LE11 3TU, UK

Reviewed, accepted September 23, 2010

Abstract

Efficient resource utilisation is seen as one of the advantages of Additive Manufacturing (AM). This paper presents a comparative assessment of electricity consumption of two major metallic AM processes, selective laser melting and electron beam melting. The experiments performed for this study are based on the production of a common power monitoring geometry. Due to the technology's parallel nature, the degree of build volume utilization will affect any power consumption metric. Therefore, this work explores energy consumption on the basis of whole builds - while compensating for discrepancies in packing efficiency. This provides insight not only into absolute levels of power consumption but also on comparative process efficiency.

Introduction

The potential impact of global warming may make a fundamental change in economic activity necessary. For the UK alone, recent figures estimate emissions of the six most important greenhouse gases at around 628.3 million tonnes of carbon dioxide equivalent (MtCO_{2e}) per year (DECC, 2010). The most significant source of greenhouse gas emissions in the UK is energy generation, creating around 219.7 MtCO_{2e} per annum. Emissions resulting directly from industrial processes contribute 16.7 MtCO_{2e}.

A potential reduction of the carbon footprint of manufacturing through the adoption of Additive Manufacturing is the subject of the ATKINS project conducted at Loughborough University. The ATKINS project is a collaborative research project funded by the UK Technology Strategy Board (TSB, 2008) and industry partners; it assesses multiple dimensions of the environmental impact of manufacturing, as defined by the Business Resource Efficiency and Waste programme (DEFRA, 2009). This includes greenhouse gas emissions, water usage, raw material consumption and the generation of hazardous waste and landfill. This paper contributes an assessment of electric energy consumption of two major metallic AM platforms, selective laser melting (SLM) and electron beam melting (EBM).

In their initial study of the environmental impact of additive systems, Luo et al. (1999) investigate the power consumption of three major polymeric AM processes: laser sintering (LS), fused deposition modelling (FDM) and stereolithography (SLA). The authors report system energy consumption in terms of an energy consumption rate, measuring kWh consumed per kg of part geometry. Tab. 1 shows the range of energy consumption rates observed by Luo et al. for the three AM variants:

SLA	LS	FDM
20.70 – 41.38 kWh/kg	29.83 – 40.09 kWh/kg	23.08 – 346.4 kWh/kg

Table 1: Ranges of energy consumption rates, Luo et al., 1999

In a similar framework, Sreenivasan and Bourell (2009) study power consumption of LS. Apart from reporting the energy consumption rate (14.5 kWh/kg), the authors also cite

mean power consumption of the investigated LS system, a 3D Systems Vanguard HS + HiQ, measured at 19.6 kWh over the investigated build. It is noteworthy that there is little research on the energy usage of the metallic variants of AM. In a cross-platform study of the effect of build parameters (such as part orientation) on AM energy consumption, Mognol et al. (2006) present power consumption estimates for the 3D Systems Thermojet 3D printer, the Stratasys FDM 3000 machine and the EOS M 250 direct metal laser sintering (DMLS) system. Tab.2 shows mean power consumption in the system's idle and busy states, as well as the minimum energy consumed to manufacture a power monitoring geometry, as reported by Mognol et al.:

	3D Printing	FDM	DMLS
Idle mean power consumption	0.69 kW	0.53 kW	2.00 kW
Busy mean power consumption	0.88 kW	0.57 kW	4.00 kW
Energy consumed per part (min.)	2.1 kWh	0.5 kWh	32 kWh

Table 2: mean power and energy consumption, Mognol et al., 1999

These figures appear to show that the DMLS process (and perhaps metallic AM in general) consumes disproportionately more energy than the non-metallic technology variants. Nevertheless, the adoption of metallic AM may result in a significant energy saving when compared to conventional manufacturing techniques and their products. Further energy savings may arise during the product life cycle of AM produced goods (see ATKINS feasibility study, 2008). These may be due to lower raw material usage, more efficient distribution methods, better part performance and improved recycling.

The goal of this study is to provide generally applicable information on electric energy consumption of modern metallic AM platforms. Power monitoring experiments were performed on an MTT SLM250 selective laser melting (SLM) system and an Arcam A1 electron beam melting (EBM) machine. A particular emphasis was placed on designing experiments and summary metrics that treat AM as a *parallel* manufacturing technology, allowing the contemporaneous production of different parts, an aspect missing from the discussed studies of AM energy efficiency. Previous models of AM input efficiency, albeit of financial inputs, describe efficient (i.e. minimum cost) technology usage only if they are performed on the basis of fully packed build volumes (Hopkinson and Dickens, 2003; Ruffo et al., 2006). This research demonstrates that the same is true in the assessment of energy inputs.

Experimental setup

For this research, a series of power monitoring experiments was conducted using a portable power monitoring setup featuring Yokogawa's CW240 digital multi-purpose power meter (for specifications, see the Yokogawa product guide, 2007). For the Arcam A1 system, power consumption was measured in a three-phase-four-wire configuration (400 V), with a total of eight probes (four current clamps and four voltage probes) connected to the system's multi phase power supply (Fig.1). However, the meter is also capable of measuring balanced and unbalanced loads in three-phase-three-wire-three-current connections.

The newest version of MTT's SLM250 operates on a single phase 240 V power supply. Hence, the power meter was set to a one-phase-two-wire configuration, with one current clamp and one voltage probe attached to both the phase and the neutral, totalling four probes.

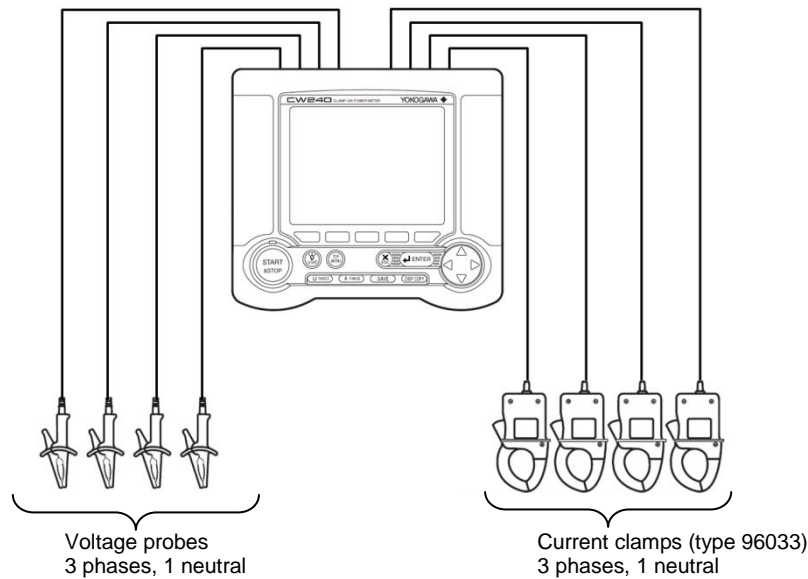


Figure 1: Three-phase-four-wire configuration, artwork taken from: User's Manual IM CW240E, Yokogawa, 2004

In the context of this study, the main variables of interest are mean real power consumption per measurement cycle (measured in W and denoted internally by the meter as 'P_AVE(W)_1'), and total cumulative energy consumed (measured in Wh and denoted as 'Wh+_INTEG(Wh)_1'). The power meter was configured to a 1s measurement cycle, this cycle length being the shortest for which all 137 measurement variables are available. Two power monitoring experiments were carried out for each AM platform:

1. In the first experiment the production of a full build volume of parts is studied, giving data on energy consumption when the machine is operating at full capacity.
2. The second experiment surveys the production of a single part located in the centre of the work space. These data were required to perform a normalisation of packing density and to analyse efficiency gains from multi-part production.

To measure total process energy consumption, the AM machines were monitored during the entire build time. Fixed process steps preceding the actual build, for example, energy expended for bed heating or vacuum drawing, are included.

An understanding of the relationships between part geometry and energy usage may be won by using a standardised power monitoring geometry. The layer-wise operating principle of the studied AM systems provides an opportunity to design a common geometry for use in such experiments. By varying the cross-sectional shape along the part's Z-axis, the effect of geometric parameters on energy consumption can be isolated. The performed power monitoring experiments use the part shown in Fig.2. This part features variation in two parameters, geometric/topological complexity and part volume.

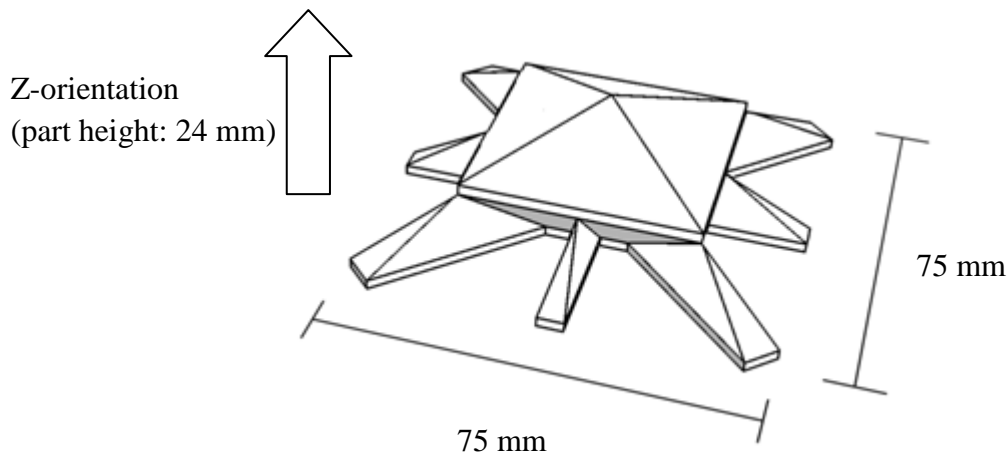


Figure 2: The standardised power monitoring geometry

In the part's lower half, the effect of geometric / topological complexity on power consumption can be assessed. This is done by varying a simple measure associated with such complexity, the ratio of cross section perimeter P and area A , along the Z axis. This also lends the part a 'spider' shaped footprint with a cavity in the centre (not visible in Fig.2). Moving up vertically, the part cross-section changes into a simple square without cavity, at a Z -height of 12 mm.

In the top half of the geometry (>12 mm Z -height), the effect of a reduction of cross section area can be studied. This is achieved by shrinking area A along the Z -axis down to a value of zero - creating a pyramidal tip. The described parameter variation can be expressed graphically, as done in Fig.3. Part cross section (solid graph) is kept relatively constant up to a Z -height of 14 mm, above which it is gradually reduced to zero. Geometric complexity (dotted graph) is reduced in the lower half of the geometry. However, this simple measure starts rising above 14 mm Z -height, due to part area A diminishing faster than the perimeter P – however, the square shape of the cross section remains, and with it the real level of complexity.

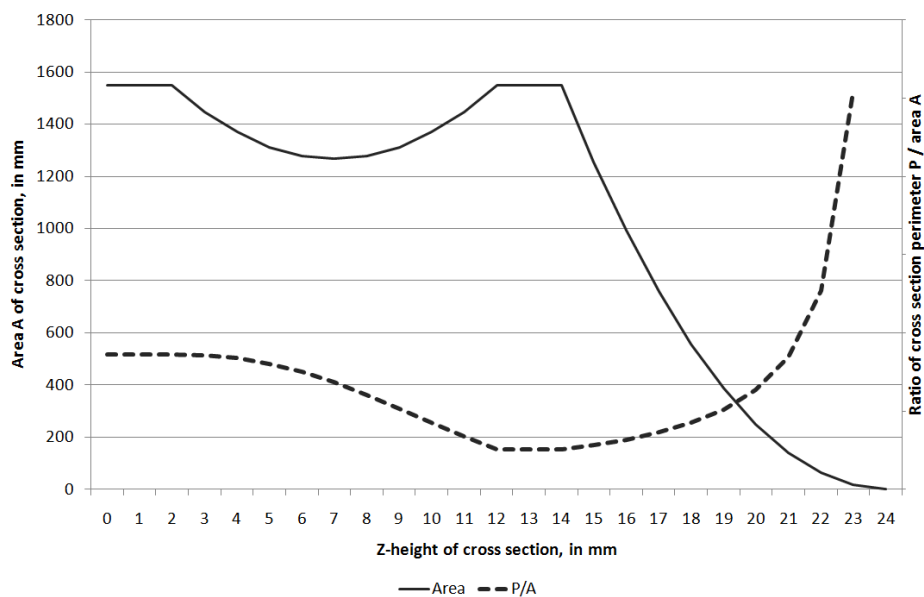


Figure 3: Variation of geometric parameters in the power monitoring geometry

While the current paper does not report the effects of geometric parameters on energy consumption, a further reason to choose the ‘spider’ shape was that it has a relatively large footprint in the X / Y dimensions. It thereby limits overall packing density, making the power monitoring builds faster and more economical. This is particularly effective for AM approaches that require every part to be attached to the build platform (referred to as 2½ dimensional build volume packing). A further consideration in the design of the part is the limitation of negative wall angles (<45°) to ensure that the investigated processes do not require supports for overhangs. Nevertheless, on some systems (such as the MTT SLM250) support structures may be required to attach the parts to a base plate.

When analysing energy consumption on the basis of full builds of identical parts, it can be expected that discrepancies in packing density arise across AM platforms, due to different build volume sizes and shapes. This makes an adjustment of the observed power consumption data necessary, which is achieved by normalising packing density. Making the simplifying assumption that for each AM system the relationship between build energy consumption and the number of parts in the build volume is linear, packing density can then be adjusted by extrapolating from the two experimental results obtained for each AM platform (full build and single part). The first step is to adjust packing density, the number of parts n parts per area A of the build platform, according to some standardised density ($n_{STANDARD}/A_{STANDARD}$):

$$n_{ADJUSTED} = n \times \frac{\frac{n_{STANDARD}}{A_{STANDARD}}}{\frac{n}{A}} \quad (1)$$

Ideally, the standard packing density would be the highest observed density in the experiments. In the sample of AM systems assessed for this paper, the Arcam A1 EBM machine featured the highest density. It should be noted that this is not indicative of system efficiency in any way; it merely shows how well the power monitoring geometries fit into a particular build volume. A corrected measure for total energy consumption during the full build experiment ($E_{ADJUSTED}$) can then be calculated using $n_{ADJUSTED}$ in conjunction with the simple intercept theorem; $E_{FULL BUILD}$ and $E_{SINGLE PART}$ denote the total energy consumed during the full build and the single part experiments:

$$E_{ADJUSTED} = \left(\frac{(n_{ADJUSTED} - 1) \times (E_{FULL BUILD} - E_{SINGLE PART})}{n_{FULL BUILD} - 1} \right) + E_{SINGLE PART} \quad (2)$$

To obtain the adjusted measure for the energy invested per part ($E_{PER PART, ADJUSTED}$), (2) is divided by $n_{ADJUSTED}$:

$$E_{PER PART, ADJUSTED} = \frac{\text{Energy consumed per build}_{ADJUSTED}}{n_{ADJUSTED}} \quad (3)$$

AM platforms investigated

The two studied variants of metallic AM share numerous features. Both operate by adding part material layer by layer in a powder bed. Nominal build volume sizes are also relatively similar, with 250 * 250 * 300 mm on the MTT SLM250 and 200 * 200 * 180 mm

on the Arcam A1. Moreover, both processes require that the manufactured parts are attached to a removable base plate. During operation, this plate is lowered by a small increment after each layer has been completed. However, the machines do exhibit significant differences. Tab. 3 summarises the most important ones in the context of this study of energy consumption:

	SLM	EBM
Machine type	MTT SLM250	Arcam A1
Power supply	240V, 8A, single phase	400V, 16A, multi phase
Beam type	IR, 1.06 μm wavelength	Electron beam
Maximum beam energy	200 W	3000 W
Nominal build volume size (X / Y / Z)	250 * 250 * 300 mm	200 * 200 * 180 mm
Used build volume size (X / Y)	230 * 230 mm	180 * 180 mm
Build material	Stainless steel, SAE 316L	Titanium, Ti-6Al-4V
Layer thickness	50 μ	80 μ
Process atmosphere	Ar, 15 mbar over normal air pressure	Vacuum, with addition of He
Powder bed temperature	~100 - 300° C	~700° C
Chiller on external power	yes	no
Parts connected to base plate through supports	yes	no
Manufacturer reference	MTT UK, 2009	Arcam AB, 2010

Table 3: Process attributes and experimental configuration

Most prominently, the energy transfer method used to selectively melt the metal powder is different. While the SLM system scans the surface with a 200 W fibre laser, transferring energy in the form of light, the EBM system melts the metal powder with an electron beam (maximum output: 3000 W). According to Strutt (1980), energy transfer efficiency by electron beam can be around 10 times greater than for certain laser types. However, this value was obtained from a comparison between electron beams and CO₂ lasers; the SLM machine employs a more efficient fibre laser operating at 1.06 μm wavelength. Thus, the comparatively lower efficiency of laser-based systems may be due to melt pool reflectivity. A drawback of using an electron beam to scan the powder bed is that this method imposes restrictions on the usable build materials, magnetic metal powders cannot be used.

The machines' process atmospheres also differ strongly. The build activity in the Arcam A1 is performed in a near vacuum (with the addition of He), drawn by a powerful turbo pump before the scanning begins. This allows a hot process, with bed temperatures of around 700° C. The high power of the electron beam, together with its efficient energy transfer, makes additional bed heating elements unnecessary – the powder bed is heated by evenly scanning the bed surface with the electron beam. In contrast to this, the MTT SLM250

operates with an Ar build atmosphere at just over normal pressure (~ 15 mbar over outside atmosphere). The process belongs to the class of ‘cold’ AM processes with bed temperatures between 100° C and 300° C. While this machine possesses build chamber heating elements, this function was deactivated during the experiments in order to run the machine at maximum energy efficiency. The MTT SLM250’s external cooling system draws power independently and had to be monitored using a second power meter. Apart from the presented measures of real power consumption, external chiller energy consumption was included in all other results presented in this paper.

In order to be reflective of machine usage in established applications, the experiments were performed with different material grades and layer thicknesses on the two machines. It was expected that the low layer thickness (50 µ) on the MTT SLM250 will result in lower process speed and higher energy consumption, due to the greater number of layers required to build the standardised power monitoring geometry. It should be noted that the advantages of small layer thicknesses, such as higher geometric tolerances and diminished surface quality, are not factored into the results presented.

Results and Discussion

Two build experiments were performed on both AM platforms, one full build experiment containing as many power monitoring geometries as possible and one build with a single part in the centre of the build platform. As expected, the packing densities for the full build volumes vary: while the build envelope of the MTT SLM250 is able to hold 6 parts, the Arcam A1 is limited to 5 power monitoring geometries. To give a concise overview, the results of the power monitoring experiments are presented in Tab. 4:

		SLM	EBM
Machine type		MTT SLM 250	Arcam A1
Number of parts in full build		6	5
Build time	Full build	1519 min (excl. supports: 1153 min)	304 min
	Single part	351 min (excl. supports: 286 min)	192 min
Mean real power consumed	Full build	1.10 kW (excl. chiller)	2.22 kW
	Single part	0.92 kW (excl. chiller)	2.01 kW
Total energy consumed	Full build	44.26 kWh	11.04 kWh
	Single part	9.14 kWh	6.41 kWh
	Parallel manufacturing factor	0.81	0.34
Summary metrics (adjusted)	Energy consumed per part	7.34 kWh	2.21 kWh
	Energy consumed per g (assuming 100% dense parts)	0.031 kWh	0.017 kWh
	Energy consumed per cm ³	0.249 kWh	0.075 kWh

Table 4: Power monitoring results

The table presents results on five different categories: part quantity, build time, real power consumption, total energy consumed and summary metrics. Of the surveyed machines, the Arcam A1 was the fastest to complete the full build experiment in 304 min, compared to 1519 min for the MTT SLM250. Subtracting the time used for the creation of the supports, the build was completed in 1153 min. The higher speed of the Arcam A1 can partially be explained by the fact that it has a smaller build volume than the MTT SLM250. Moreover, it operates with an effective electron beam scanning system without moving parts, capable of high scan speeds. Another factor of particular importance is that layer thickness on the Arcam A1 (80 μ) is 1.6 times larger than on the MTT SLM250 (50 μ). It should also be noted that the supports connecting the parts to the platform were not optimised for the MTT SLM250, resulting in a further slowdown of build speed.

The measured mean real power consumption describes the average amount of AC power the machine is consuming over the course of the build, including any fixed heating up, atmosphere generation and cooling down procedures. The power supply specification is chosen by the manufacturers based on this characteristic. However, this measure is not very helpful in the analysis of AM energy efficiency as it omits process time and productivity. Nevertheless, existing studies on AM energy efficiency report this result (Mognol et al., 2006; Sreenivasan and Bourell, 2009). The values observed during the current research appear significantly lower than the results presented in the literature. Mognol et al. report an average build time power consumption of 4.00 kW for the (now obsolete) EOS M 250 DMLS system, this appears high compared to an energy consumption of 1.10 kW for the MTT SLM250, which is technologically similar.

Total energy consumption is a more applicable measure of true process efficiency, in particular when recorded for a full build. In the performed experiments, both in the full build and in the single part experiments, the Arcam A1 showed the lowest total energy expenditure (11.04 and 6.41 kWh). As discussed above, this is not surprising considering the smaller build volume and the high layer thickness. Furthermore, EBM uses titanium (Ti-6Al-4V) as raw material. Titanium has a lower density than steel, combined with a roughly similar specific heat capacity (~ 0.5 kJ/kg K). It should be noted that titanium has a higher melt point and a different energy absorption rate than steel. Measuring total energy consumption allows the calculation of a statistic reflecting the energy savings available through the contemporaneous production of multiple parts, labelled the ‘parallel manufacturing factor’:

$$\textit{Parallel manufacturing factor} = \frac{E_{FULL BUILD} / n}{E_{SINGLE PART}} \quad (4)$$

This factor gives an indication of the effect on energy consumption of parallel production of multiple parts. It shows how well the energy investment associated with the process can be amortised over multiple parts included in each build. A low value indicates that the savings available from parallel production are large: the factor of 0.34 recorded for the Arcam A1 implies that if multiple parts are manufactured per build instead of one, only 34 % of the energy needs to be invested per part. With a parallel manufacturing factor of 0.81, the MTT SLM250 offers lower energy savings of this kind. A more powerful laser, faster scanning and a larger build volume could improve this value, however.

Appreciating the discussed impact of packing density, summary metrics (based on full build energy consumption) are reported in adjusted form. Information on the following three metrics is reported: energy consumption per part, energy consumed per g and energy consumed per cm³ of part volume. In terms of energy consumption per part, the results show that the SLM process consumes around 7.34 kWh while the EBM process uses around 2.21 kWh. Keeping in mind that differences in material, layer thickness and surface quality may account for this, it appears that the Arcam A1 consumes around 70% less energy per part than the competing SLM process. This is surprising as mean real power consumption of EBM is much higher (2.22 kW vs. 1.10 kW without chiller). In terms of overall energy consumption, though, this is more than offset by a higher process speed (304 min vs. 1519 min). The measure for energy consumed per g of part volume is based on fully dense parts, assuming a density of 8.00 g / cm³ for the parts produced in stainless steel grade SAE 316L on MTT's SLM250 and 4.43 g / cm³ for the Ti-6Al-4V parts from the Arcam A1. This summary metric can be used to mimic the energy consumption rates of AM systems in the literature, as reported for polymeric LS by Luo et al. (1999) and Sreenivasan and Bourell (2009):

	Lou et al. (1999)	Sreenivasan and Bourell (2009)	This research	
System type	DTM Sinterstation 2000, Sinterstation 2500	3DS Vanguard HiQ+HS	MTT SLM250	Arcam A1
Process class	LS	LS	SLM	EBM
Material	Polyamide	Polyamide	SAE 316L	Ti-6Al-4V
Energy consumption rate	40.09 kWh / kg , 29.83 kWh / kg	14.5 kWh / kg	31 kWh / kg	17 kWh / kg

Table 5: Energy consumption rates for AM systems

Even though the processes analysed for this research generate metal parts and the previous work focuses on polymeric AM, the obtained results roughly fall in line with the published energy consumption levels for LS. However, the discrepancy between this result and the observation that metallic AM consumes more energy than polymeric AM (Mognol et al., 2006) suggests that more research is needed.

Conclusions

The comparative assessment of electricity consumption of the SLM and EBM processes demonstrates that studies on input efficiency for parallel manufacturing systems can lead to different results if full build volumes are considered instead of one-off parts. This will be particularly relevant for systems exhibiting a low parallel manufacturing factor, as defined above (4). The single part build experiment on the Arcam A1 (factor 0.39) resulted in an energy investment of 6.41 kWh, compared to an adjusted full build energy consumption per part of 2.21 kWh. For the MTT SLM250 (factor 0.81), the picture is similar but not as pronounced: the single build required in an energy investment of 9.14 kWh, compared to an adjusted full build energy consumption per part of 7.34 kWh.

It has also been demonstrated that a standardised testing part can lead to meaningful results in full build studies of AM energy consumption. An important step is, however, to

compensate for differences in packing density. This ensures that results that are not distorted by indivisibilities resulting from fixed part size.

The lower energy consumption measured for the EBM platforms appears to be, at least partially, due to differences in material and layer thickness. While the specific heat capacities of stainless steel and titanium are similar, the density of titanium is much lower. Hence, to heat a volume measure by 1° C, steel requires more energy. Moreover, the presented metrics do not reflect the advantages of a low layer thickness - such as improved surface finish and tighter dimensional tolerances. For future studies, it would be advisable to compensate for variations in layer thickness. Furthermore, it should be noted that this study has not dealt with part supports in a systematic way. Unlike the experiments performed on the Arcam A1, the experiments performed on the MTT SLM250 included substantial support structures connecting the parts to the base plate (created using the Marcam AutoFab package).

In the context of the ATKINS project, it will be important to substantiate claims that AM is a more energy efficient alternative to conventional manufacturing. This can be done by comparing summary metrics, such as kWh/cm³ or kWh/g, to corresponding data collected for conventional manufacturing processes

Acknowledgements

The authors would like to use this opportunity to express their gratitude to the following individuals who have expertly performed the build experiments. The experiments took place at several locations: at the AMRG at Loughborough University (UK), thanks go to Mark Hardy; at Arcam AB (Gothenburg, Sweden), the authors thank Dr. Ulric Ljungblad, Isak Elfström and Daniel Jonasson; and at MTT Technologies Group (Stone, UK) where the authors thank Dr. Chris Sutcliffe, Kevin Hart and Paul Smith for their support.

References

- Arcam AB, 2010. *Arcam A1 – The future in implant manufacturing*. [Online]. Available from: <http://www.arcam.com/CommonResources/Files/www.arcam.com/Documents/Products/Arcam-A1.pdf> [Accessed: 15.06.2010]
- *ATKINS feasibility study*. Downloads, 2008. [Online]. Available from: <http://atkins-project.com/web/atkins/pdf/ATKINSfeasibilitystudy.pdf> [Accessed: 28.01.2009].
- DECC, 2010. *UK climate change sustainable development indicator: 2008 greenhouse gas emissions, final figures*. [Online]. Available from: http://www.decc.gov.uk/en/content/cms/statistics/climate_change/gg_emissions/uk_emissions/uk_emissions.aspx [Accessed: 01.07.2010.]
- DEFRA, 2009. *Business Resource Efficiency and Waste (BREW) Programme, Disaggregated Metrics Results for 2006/07*. [Online] Available from <http://www.defra.gov.uk/environment/business/support/results.htm> [Accessed:08.07.2010]
- Hopkinson, N, and Dickens, P., 2003. Analysis of rapid manufacturing – using layer manufacturing processes for production. *Proceedings of IMechE Part C: Journal of*

Mechanical Engineering Science, 217 (1), pp.31-39.

- Luo, Y., Ji, Z., Leu, M. C., and Caudill, R., 1999. Environmental Performance Analysis of Solid Freeform Fabrication Processes. *Proceedings of the 1999 IEEE International Symposium on Electronics and the Environment*, pp 1-6.
- Mognol, P., Lopicart, D., and Perry, N., 2006. Rapid prototyping: energy and environment in the spotlight. *Rapid Prototyping Journal*, 12 (1), pp.26-34.
- MTT Technologies Group UK, 2009. *MTT Selective Laser Melting*. [Online]. Available from: http://www.mtt-group.com/data/pdf/extract/0413-MTT_2pp_SLM_A4_%20Flyer_v1.pdf [Accessed: 16.06.2010]
- Ruffo, M., Tuck, C., and Hague, R., 2006. Cost estimation for rapid manufacturing – laser sintering production for low to medium volumes. *Proceedings of IMech E Part B: Journal of Engineering Manufacture*, 220 (9), pp.1417-1427.
- Sreenivasan, R., and Bourell, D. L., 2009. Sustainability Study in Selective Laser Sintering. *Proceedings of the 2009 Solid Freeform Fabrication Symposium*. University of Texas at Austin.
- Strutt, P. R., 1980. A Comparative Study of electron Beam and Laser Melting of M2 Tool Steel. *Materials Science and Engineering*, 44 (1), pp.239-250.
- Technology Strategy Board (TSB), 2008. *Atkins Project*, ProjRef TP/N0012J.
- Yokogawa Electric Corporation, 2007. *All Products Guide V.11*. [Online]. Available from: http://tmi.yokogawa.com/files/uploaded/BU00A02B02_60E_4.pdf [Accessed: 11.06.2010]
- Yokogawa Electric Corporation, 2004. *User's Manual IM CW240E*. Tokyo: Yokogawa Electric Corp.